

SAW Synthesis With IDTs Array and the Inverse Filter: Toward a Versatile SAW Toolbox for Microfluidics and Biological Applications

Antoine Riaud, Michael Baudoin, Jean-Louis Thomas, and Olivier Bou Matar

Abstract—Surface acoustic waves (SAWs) are versatile tools to manipulate fluids at small scales for microfluidics and biological applications. A nonexhaustive list of operations that can be performed with SAW includes sessile droplet displacement, atomization, division, and merging but also the actuation of fluids embedded in microchannels or the manipulation of suspended particles. However, each of these operations requires a specific design of the wave generation system, the so-called interdigitated transducers (IDTs). Depending on the application, it might indeed be necessary to generate focused or plane, propagating or standing, and aligned or shifted waves. Furthermore, the possibilities offered by more complex wave fields such as acoustical vortices for particle tweezing and liquid twisting cannot be explored with classical IDTs. In this paper, we show that the inverse filter technique coupled with an IDTs array enables us to synthesize all classical wave fields used in microfluidics and biological applications with a single multifunctional platform. It also enables us to generate swirling SAWs, whose potential for the on-chip synthesis of tailored acoustical vortices has been demonstrated lately. The possibilities offered by this platform are illustrated by performing many operations successively on sessile droplets with the same system.

Index Terms—Acoustofluidics, inverse filter, microfluidics, surface acoustic wave (SAW).

I. INTRODUCTION

SINCE the seminal work of Shiokawa *et al.* in 1989 on the atomization of droplets [1], the potential of surface acoustic waves (SAWs) for fluid actuation at microscale has been widely explored in the literature: progressive waves synthesized by straight interdigitated transducers (IDTs) enable sessile droplets displacement [2]–[5] or fluid pumping in a microchannel [6], [7]. Acoustic fields generated by pairs of IDTs can be combined to synthesize stationary waves and manipulate collectively particles [8]–[15], or cells [10], [16]–[21] in droplets or embedded in a

microfluidic chamber. Focused waves synthesized by concentric IDTs are suitable for the fusion of droplets [22] or for high-power applications such as droplet atomization [23]. Finally, more complex operations such as mixing at low Reynolds number through chaotic advection or droplet division may require some fancy combination of plane waves with either rotating [24] or shifted [25] wavefronts. So far, it has thus been demonstrated that SAWs enable to perform many basic operations required in microfluidics and biological applications [26], [27].

Nevertheless, each of these operations requires a specific optimized design, which is not compatible with a multifunctional actuation platform required for the development of many labs-on-chips. One strategy developed recently to perform several operations with a single transducer is to use phononic crystal superstrates to shape the acoustic field [28], [29]. Nevertheless, only a limited number of operations can be obtained with these systems. Moreover, neither classical IDTs nor superstrates allow the synthesis of swirling SAWs [30] envisioned for the on-chip synthesis of tailored acoustical vortices [31] and consequently, 3-D single particle manipulation [32] and vorticity control [33]. To overcome these shortcomings, we developed an array of 32 optimized IDTs driven by a programmable electronics that enables independent control of each transducer. To synthesize the targeted wave field, the inverse filter technique [34] originally developed for bulk waves has been adapted for SAWs [30]. In this paper, we show that it is possible to synthesize plane waves in different directions, focused waves with the focal point located at an arbitrary position, and swirling SAWs with the same device. The potential of this system is illustrated on sessile droplets by showing successively droplet controlled displacement, division, fusion, and nebulization with the same platform.

II. METHODS

Rayleigh SAWs (R-SAWs) are synthesized at the surface of an X-cut, 1.05-mm thick, niobate lithium (LiNbO₃) piezoelectric substrate by an array of 32 unidirectional IDTs (SPUDT IDTs) (see Fig. 1). The X-cut was chosen for its good electromechanical coefficients along the z ($K^2 = 5, 9\%$) and y ($K^2 = 3, 1\%$) directions and its weaker anisotropy compared with the 128° Y-cut generally used for unidirectional IDTs. The IDTs array (IDTA) was fabricated using a liftoff process.

Manuscript received December 24, 2015; accepted April 21, 2016. Date of publication April 27, 2016; date of current version October 1, 2016. This work was supported by the Agence Nationale de la Recherche under Grant ANR-12-BS09-0021-01 and Grant ANR-12-BS09-0021-02 and Region Nord Pas de Calais. (Corresponding author: Michael Baudoin.)

The authors are with the Institut d'Electronique, de Microelectronique et de Nanotechnologie, LIA LICS, Université de Lille and École Centrale de Lille, Villeneuve d'Ascq 59652, France, and also with the Institut des Nanosciences de Paris, Sorbonne Universités, Université Pierre et Marie Curie, Paris 75005, France (e-mail: antoine.riaud@insp.jussieu.fr; michael.baudoin@univ-lille1.fr; jean-louis.thomas@upmc.fr; olivier.boumatar@iemn.univ-lille1.fr).

Digital Object Identifier 10.1109/TUFFC.2016.2558583

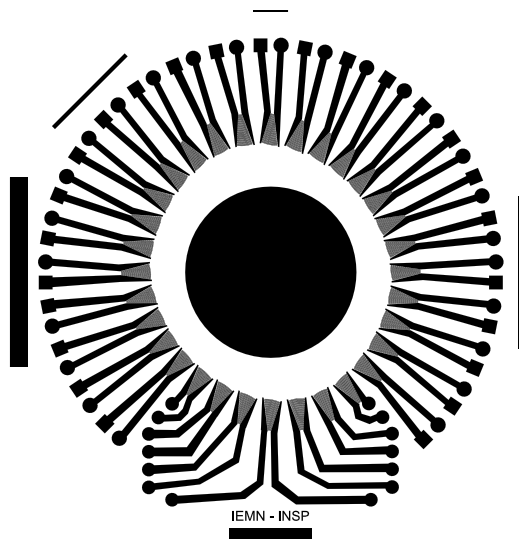


Fig. 1. Optimized array of 32 interdigitated unidirectional transducers used for the synthesis of various SAW-fields (focused, plane, swirling) and the manipulation (displacement, division, fusion, atomization) of droplets. The central black zone is a gold layer used as a mirror for the measurement of the transducer response with the Michelson interferometer. The straight lines around the system correspond to the alignment marks used to keep track of the orientation of the lithium niobate crystal along the fabrication process.

- 1) The substrate is coated with an AZ15-10 photoresist sacrificial layer patterned with the conventional photolithography technique.
- 2) A titanium (Ti) layer of 20 nm and a gold (Au) layer of 200 nm are deposited by evaporation (titanium is used for its good adherence on LiNbO₃ and gold for its good electrical conductivity).
- 3) The sacrificial layer is washed out by a developer.

The IDTA has been designed for a working frequency of 11.9 MHz, with a wavelength adapted to each wave propagation direction of the anisotropic LiNbO₃ crystal. Compared with [30], the design has been further optimized by placing the IDTs on a slowness curve and slightly curving the IDTs to promote diffraction. Each curved IDT is designed as a truncated annular transducer described in [35]. The diffraction pattern of the transducers can be estimated from the (far-field) Green function provided in [35]. We proceeded iteratively to find the optimal aperture of the IDT. We placed each IDT along the wave surface of the substrate to compensate for beam stirring. These two modifications improve the illumination by each transducer of the central zone (radius of 5 mm) of the substrate that we call the acoustical scene and where microfluidic operations are performed. An optimal spatial coverage is indeed essential for the synthesis of a wide variety of acoustic wave fields.

Each of the IDTs is excited independently with a dedicated programmable electronics that enables the synthesis of wave packets at carrying frequencies up to 12 MHz. Impedance matching for each transducers was achieved with external electronic components (inductances). Finally, the inverse filter method [34] was used to determine the optimal input signal for each IDT to synthesize a targeted wave field. Indeed, the

inverse filter is a very general method to synthesize a specific wave field in a linear medium given a set of independent programmable sources. This process can be basically decomposed into three distinct stages. First, the signal emitted by each transducer (impulse response) is measured in the acoustics scene. In practice, this response is recorded in a number of control points whose distance cannot exceed $\lambda/2$ according to the Nyquist–Shannon sampling principle. This allows to define, in the Fourier space, a transfer matrix $H_{ij}(\omega)$ (called the propagation operator) between the Fourier transform of the entrance signal emitted by transducer j , $E_j(\omega)$, and the response signal at control point i , $S_i(\omega)$: $S_i = H_{ij}E_j$ (with Einstein notations). In the present experiments, the surface vibrations of the substrate at control point i (typically of the order of a few nanometers) are measured by a home-made polarized Michelson interferometer whose principle is given in [30]. Then, the targeted output signal S is defined and the transfer matrix H is inverted to compute the optimal input signal $E = H^{-1}S$. Finally, the optimal signal is synthesized by each transducer. If $e_j(t)$, $s_i(t)$, and $h_{ij}(t)$ are the inverse Fourier transforms of $E_j(\omega)$, $S_i(\omega)$, and $H_{ij}(\omega)$, it is worth noting that the output time signal $s(t)$ is the convolution product of $h_{ij}(t)$ and $e_j(t)$

$$s_i(t) = h_{ij}(t) * e_j(t).$$

While the inverse filter method is simple in principle, some complexity arises when implementing it. Indeed, the propagation operator is generally ill-conditioned since small errors in the measurements produce very large errors in the reconstructed results. Then, the number of control points is not necessarily the same as the number of sources (transducers) and thus the propagation operator is not necessarily a square matrix. So, the pseudoinverse of the propagation operator is obtained through singular value decomposition. Finally, the inverse filter technique had been initially developed to generate acoustical wave fields in 3-D media. In this case, the target field is a surface and has a smaller dimensionality (2-D) than the propagative medium (3-D), whereas for SAWs, the target field has the same dimensionality as the propagative medium (both 2-D). So the control points are not independent and the wave field must fulfill the dispersion relation. This requires some refinements in the method (see [30]).

To enable droplet manipulation, the central zone was treated with a hydrophobic self-assembled monolayer [36]. Otherwise, the droplet would spread on the gold layer at the center of the niobate lithium substrate, since it is a perfect wetting medium. Nevertheless, the adherence of alkane-thiol molecules on the central gold layer was not optimal leading to a contact angle below 90° ($\theta \approx 70^\circ$), large hysteresis, and thus pinning of the contact line. Despite these bad properties of the hydrophobic layer, we nevertheless succeeded to control the drop displacement with the IDTA as we will see in the following section. The droplet dynamics was recorded with a Pointgrey Flea 3 camera on an MZ1 Viewsolution microscope at 75 frames/s. A sketch of the experimental setup is shown in Fig. 2.

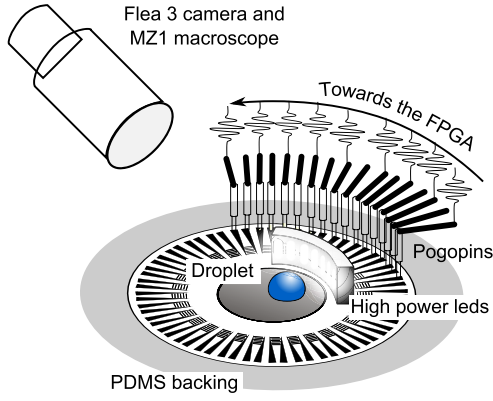


Fig. 2. Sketch of the experimental setup used for the synthesis of various wave fields and the actuation of droplets.

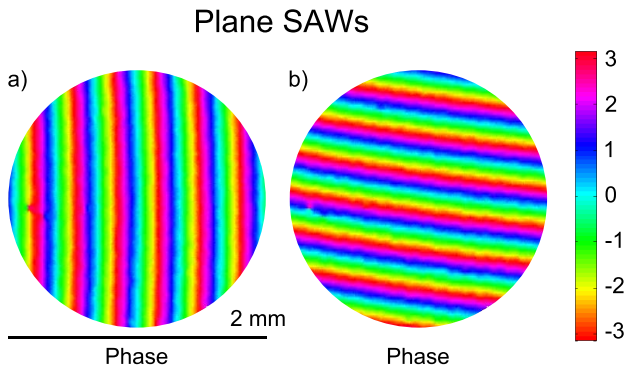


Fig. 3. (a) and (b) Phase of plane progressive SAWs synthesized with the IDTA in two different directions. The maximum peak-to-peak amplitude in the two directions are, respectively, 6 and 10 nm.

III. RESULTS

A. Complex Wave Fields Synthesis

To demonstrate the potential of the SAW toolbox for fluid sample actuation, we first investigated the possibilities offered by the IDTA and the inverse filter technique to synthesize the main SAW-fields used in the literature: plane, focalized, and swirling SAWs.

While our setup is optimized for the synthesis of focalized waves and swirling SAWs (since the IDTs are disposed radially around the slowness curve), we have shown that it is possible to synthesize waves with plane wavefronts in the desired direction with peak-to-peak amplitudes larger than 5.5 nm, that is to say, well above the values classically used for droplets displacement [4], [5]. We provide in Fig. 3 two examples of plane progressive waves synthesized in different directions. These results show that despite the curvature of the IDTs, the wavefront aberration is weak in the acoustical scene and is compensated by the inverse filter.

Then, we synthesized focalized waves with different positions of the focal point in the acoustical scene and apodization around a preferential direction ϕ_0 (see Fig. 4). It is important to note that contrary to previous attempts to synthesize focalized waves for microfluidic applications with concentric IDTs [26], the anisotropy of the piezoelectric medium

Focalized anisotropic SAWs

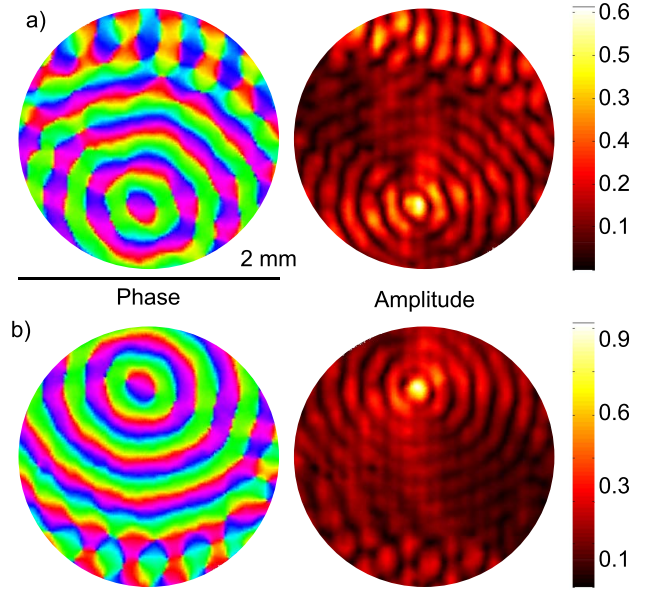


Fig. 4. (a) and (b) Phase and amplitude of focalized propagative anisotropic SAWs converging at two different focal points. The maximum peak-to-peak amplitude for the two different focal points are, respectively, 60 and 100 nm. Colorbar: peak-to-peak amplitude $\times 10^{-2}$ nm.

is considered here in the definition of the targeted wave field

$$\mathcal{F}(r, \theta) = \frac{1}{2\pi} \int_{-\pi}^{\pi} h(\phi - \phi_0, \sigma) e^{ik_r(\phi)r \cos(\phi-\theta)} d\phi$$

with

$$h(\phi - \phi_0, \sigma) = \exp \left[-\frac{\|\phi - \phi_0\|^2}{4\pi^2 \sigma^2} \right]$$

(r, θ) the polar coordinates, $k_r(\phi) = \omega/c_R(\phi)$, the radial wave vector, $c_R(\phi)$, the phase speed of R-SAWs in the ϕ direction (defining the anisotropy of the medium, σ the aperture (here $\sigma^2 = 0.2$) and the symbol $\|\cdot\|$ denotes the shorter angular distance [which can be computed as follows $\|\phi - \phi_0\| = \arccos(\cos(\phi - \phi_0))$). The function h then represents an apodization over an aperture σ .

Consideration of the anisotropy is indeed essential to ensure real focalization of the acoustic wave. Excellent results are obtained (see Fig. 4) with the maximum normal amplitude of the R-SAW of up to 100 nm. Naturally, small discrepancies are observed compared with the targeted wave field (the phase does not exactly follow the slowness curve) owing 1) to the finite numbers of transducers used for the field synthesis and 2) to the finite number of measurement points obtained with the interferometer and used for the reconstruction of the experimental acoustic field.

Finally, anisotropic swirling SAWs of the topological order 0 and 2 have been synthesized with the new transducers array presented in this paper (see Fig. 5). The targeted wave field is defined according to the formula introduced in [30]

$$\mathcal{W}_l(r, \theta) = \frac{1}{2\pi i^l} \int_{-\pi}^{+\pi} e^{il\phi + ik_r(\phi)r \cos(\phi-\theta)} d\phi \quad (1)$$

Anisotropic swirling SAWs

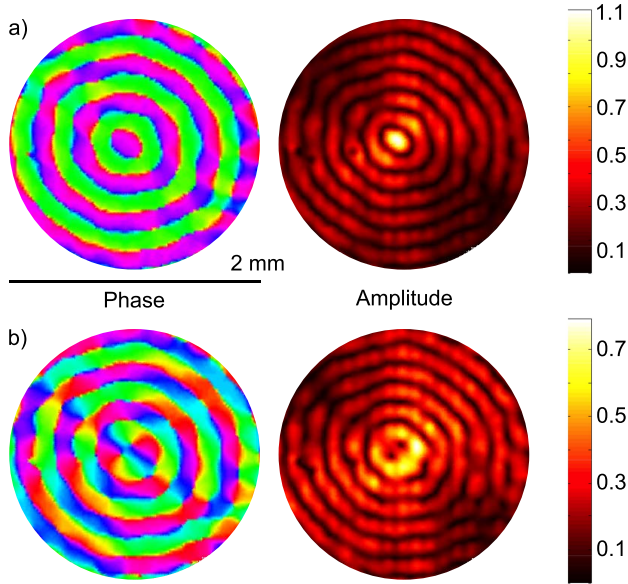


Fig. 5. (a) and (b) Phase and amplitude of anisotropic swirling SAWs of topological order 0 and 2. The maximum peak-to-peak amplitude of the \mathcal{W}_0 and \mathcal{W}_2 swirling SAWs are, respectively, 108 and 80 nm. Colorbar: peak-to-peak amplitude $\times 10^{-2}$ nm.

with l as the topological order of the swirling SAW. It is interesting to note that swirling SAWs of order 0 are nothing but focalized waves with no angular apodization. These waves are not appropriate for particle tweezing or vorticity control since they do not have phase singularity (and thus dark spot) at their center to trap particles and they do not carry angular momentum contrary to higher order swirling SAWs. Nevertheless, they can be of much practical use for applications where high intensity is required at the focal point.

B. Droplet Manipulation With the Platform

These specific wave fields have been used to perform operations on water droplets of initial volume $2 \mu\text{l}$. Since it is not possible to synthesize continuous wave fields with the programmable electronics, some burst of duration $25 \mu\text{s}$, carrying frequency 11.9 MHz and variable repetition rates of a few kilohertz have been used for droplet actuation (for each operation, the exact sequence used for actuation is described in the corresponding figure). Since droplet displacement is the result of cumulative nonlinear effects (radiation pressure and acoustic streaming), and the characteristic hydrodynamic times associated with droplets motion are slow compared with the repetition rates, the forcing is essentially seen as a continuous forcing. Nevertheless, the repetition rates of several kilohertz are compatible with droplets of high-order inertio-capillary vibrations [5], [37]–[39], which may explain why spurious atomization of the drop has been observed. Indeed, both the frequency of the excitation and the acoustical powers used in the present experiments are compatible with droplet nebulization [38] (larger power than usual was used in the present experiments to overcome the retention of the contact line). Nevertheless, this shortcoming could be simply overcome with

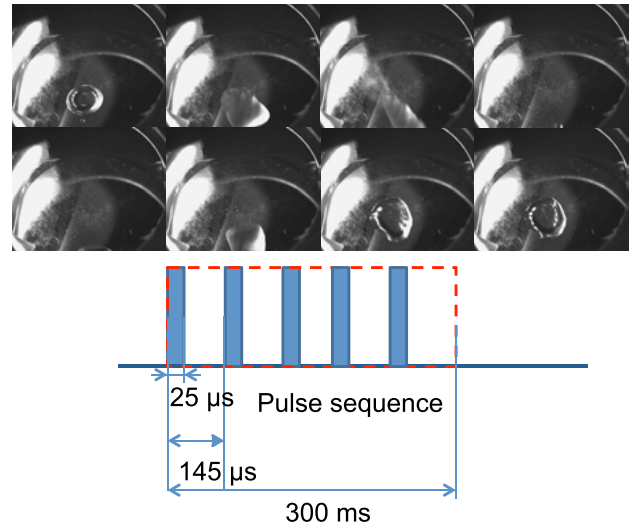


Fig. 6. Stack of images showing the displacement forward and backward of a $2\text{-}\mu\text{l}$ droplet in the acoustical scene. The displacement is obtained with focalized waves propagating successively in the opposite directions. The time elapsed between two successive images is 53 ms. See also S1.

appropriate hydrophobic treatment of the surface with low hysteresis [40].

Droplet displacement (Fig. 6, S1), fusion (Fig. 7, S3) and atomization (Fig. 8, second part of S3) were obtained, respectively, with focalized waves, swirling SAWs of second and zero order. The characteristics of the wave field are summarized in the corresponding figure. For the droplet division (Fig. 9, S2), we used a different method than the one proposed in [25]: we alternatively synthesized some burst of focalized waves with two different focal points as presented in the previous section. With this specific wave field, we were able to separate droplets even at such high contact line hysteresis.

IV. DISCUSSION

In this paper, we have shown that the combination of IDTA and the inverse filter technique enables the synthesis of the most common SAW-fields used for actuation of fluids at the microscale: plane waves in different directions, anisotropic focalized SAWs, and anisotropic swirling SAWs. As a proof of concept, we show that this SAW toolbox enables to perform many basic operations required in droplet-based digital microfluidics: droplet displacement, division, fusion, and atomization. Since it is virtually possible to synthesize any acoustic wave field compatible with the anisotropy of the substrate, it might be easily demonstrated that it is possible to perform other operations previously demonstrated in the literature such as micromixing, collective particle manipulation with standing waves, or jetting. In the same way, it might be possible to demonstrate the versatility of this platform for fluid sample manipulations in microchannels.

The most thrilling perspectives of this SAW toolbox nevertheless lie in the development of new operations that cannot be achieved with other techniques, such as selective 3-D manipulation of one or a few particles or cells (displacement, rotation), precise vorticity control independent of

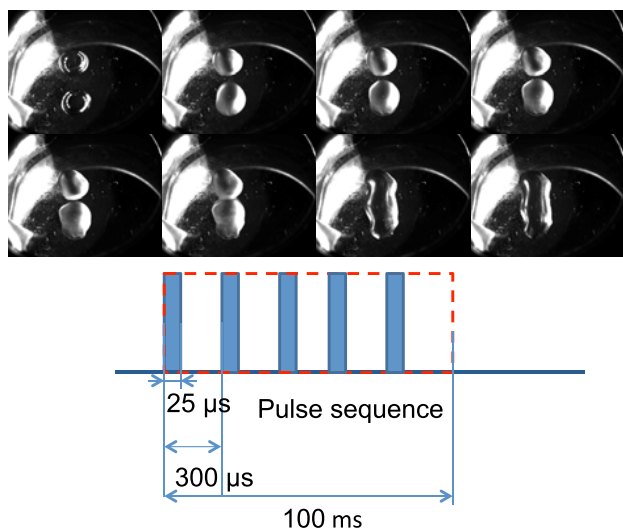


Fig. 7. Stack of images showing the fusion of two droplets of $2\ \mu\text{l}$. The fusion is obtained with centered swirling SAWs of topological order 2. The time elapsed between two successive images is 27 ms. See also S3.

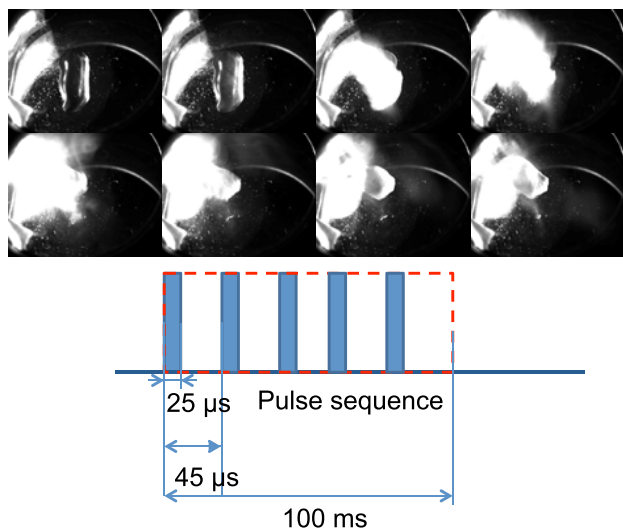


Fig. 8. Stack of images showing the atomization (nebulization) of a $2\text{-}\mu\text{l}$ droplet. It is obtained with a high intensity centered swirling SAW of order 0 (annular wave). The time elapsed between two successive images is 13 ms. See also second part of S3.

the boundary conditions with swirling SAWs, or collective manipulation of several sessile droplets. This last operation is indeed not possible with a limited number of transducers, since 1) there is a shadow zone behind each droplet that prevents the displacement of a second droplet situated behind it due to the strong absorption of Rayleigh waves by liquid samples, and 2) it would be necessary to localize the droplets position in real time. These problems could be overcome with IDTA and the inverse filter method. Indeed, the combination of the acoustic waves emitted by each transducer enables better spatial coverage of the substrate and the inverse filter method allows adaptive focusing in the heterogeneous and absorbing media [41], [42]. The procedure would thus consist of the following.

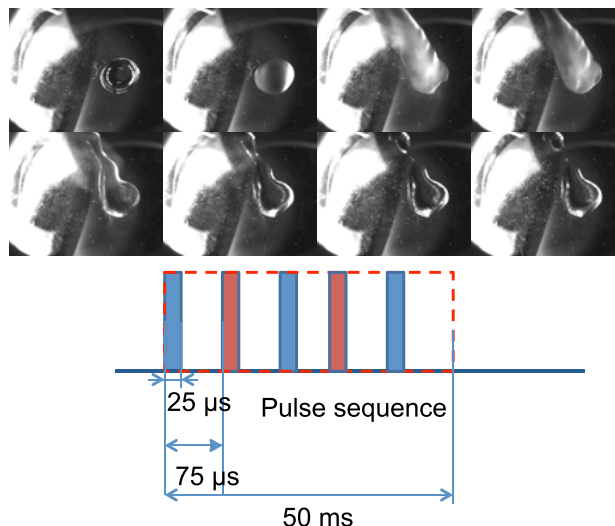


Fig. 9. Stack of images showing the asymmetric division of a $2\text{-}\mu\text{l}$ droplet into two daughter droplets of different volumes. It is obtained with waves focalized at two focal points situated on both sides of the drops and with an angular apodization. The time elapsed between two successive images is 27 ms. See also S2. Blue and red pulses represent successive pulses of focalized waves at different positions and directions as shown in Fig. 4.

- 1) Acquiring a set of databanks of impulse responses for the substrate and the shadowing droplet.
- 2) Using the inverse filter method to determine which signal must be produced by the IDTA to get the targeted signal for the second drop, depending on its relative position compared with the shadowing drop.
- 3) Using the IDTA as sensors to localize in real time both droplets with either an echo [3] or a transmission method [43], [44].

This work opens prospects toward the design of potentially the most versatile toolbox for active control of small fluid samples, for microfluidics and biological applications.

ACKNOWLEDGMENT

The authors would like to thank Pr. J. R. Friend and Pr. D. W. Greve for their invitation to the IEEE International Ultrasonic Symposium 2015 in Taipei that enabled their group to present these results.

REFERENCES

- [1] S. Shiokawa, Y. Matsui, and T. Ueda, "Liquid streaming and droplet formation caused by leaky Rayleigh waves," in *Proc. IEEE Ultrason. Symp.*, vol. 1, Oct. 1989, pp. 643–646.
- [2] A. Wixforth, C. Strobl, C. Gauer, A. Toegl, J. Scriba, and Z. V. Guttenberg, "Acoustic manipulation of small droplets," *Anal. Bioanal. Chem.*, vol. 379, no. 7, pp. 982–991, Aug. 2004.
- [3] A. Renaudin, P. Tabourier, V. Zhang, J. C. Camart, and C. Druon, "SAW nanopump for handling droplets in view of biological applications," *Sens. Actuators B, Chem.*, vol. 113, no. 1, pp. 389–397, Jan. 2006.
- [4] P. Brunet, M. Baudoin, O. Bou Matar, and F. Zoueshtigh, "Droplet displacements and oscillations induced by ultrasonic surface acoustic waves: A quantitative study," *Phys. Rev. E*, vol. 81, p. 036315, Mar. 2010.

- [5] M. Baudoin, P. Brunet, O. Bou Matar, and E. Herth, "Low power sessile droplets actuation via modulated surface acoustic waves," *Appl. Phys. Lett.*, vol. 100, no. 15, p. 154102, 2012.
- [6] S. Girardo, M. Cecchini, F. Beltram, R. Cingolani, and D. Pisignano, "Polydimethylsiloxane-LiNbO₃ surface acoustic wave micropump devices for fluid control into microchannels," *Lab Chip*, vol. 8, no. 9, pp. 1557–1563, 2008.
- [7] M. Cecchini, S. Girardo, D. Pisignano, R. Cingolani, and F. Beltram, "Acoustic-counterflow microfluidics by surface acoustic waves," *Appl. Phys. Lett.*, vol. 92, no. 10, p. 104103, 2008.
- [8] R. Shilton, M. K. Tan, L. Y. Yeo, and J. R. Friend, "Particle concentration and mixing in microdrops driven by focused surface acoustic waves," *J. Appl. Phys.*, vol. 104, no. 1, p. 014910, 2008.
- [9] J. Shi, X. Mao, D. Ahmed, A. Colletti, and T. J. Huang, "Focusing microparticles in a microfluidic channel with standing surface acoustic waves (SSAW)," *Lab Chip*, vol. 8, no. 2, pp. 221–223, 2008.
- [10] J. Shi, D. Ahmed, X. Mao, S.-C. S. Lin, and T. Huang, "Acoustic tweezers: Patterning cells and microparticles using standing surface acoustic waves (SSAW)," *Lab Chip*, vol. 9, no. 20, pp. 2890–2895, 2009.
- [11] R. Raghavan, J. Friend, and L. Yeo, "Particle concentration via acoustically-microcentrifugation," *Microfluidics Nanofluidics*, vol. 8, pp. 73–84, May 2010.
- [12] S. B. Q. Tran, P. Marmottant, and P. Thibault, "Fast acoustic tweezers for the two-dimensional manipulation of individual particles in microfluidic channels," *Appl. Phys. Lett.*, vol. 101, no. 11, p. 114103, 2012.
- [13] X. Ding *et al.*, "On-chip manipulation of single microparticles, cells, and organisms using surface acoustic waves," *Proc. Nat. Acad. Sci. USA*, vol. 109, no. 28, pp. 11105–11109, 2012.
- [14] J. Guo, J. L. W. Li, Y. Chen, L. Y. Yeo, J. R. Friend, and Y. Kang, "RF-activated standing surface acoustic wave for on-chip particle manipulation," *IEEE Trans. Microw. Theory Techn.*, vol. 62, no. 9, pp. 1898–1904, Sep. 2014.
- [15] D. J. Collins, T. Alan, and A. Neild, "The particle valve: On-demand particle trapping, filtering, and release from a microfabricated polydimethylsiloxane membrane using surface acoustic waves," *Appl. Phys. Lett.*, vol. 105, no. 3, p. 033509, 2014.
- [16] T. Franke, S. Braunmüller, L. Schmid, A. Wixforth, and D. A. Weitz, "Surface acoustic wave actuated cell sorting (SAWACS)," *Lab Chip*, vol. 10, no. 6, pp. 789–794, 2010.
- [17] A. Hartmann *et al.*, "A novel tool for dynamic cell adhesion studies—The de-adhesion number investigator DANI," *Lab Chip*, vol. 14, no. 3, pp. 542–546, 2014.
- [18] N. Sivanantha *et al.*, "Characterization of adhesive properties of red blood cells using surface acoustic wave induced flows for rapid diagnostics," *Appl. Phys. Lett.*, vol. 105, no. 10, p. 103704, 2014.
- [19] X. Ding *et al.*, "Cell separation using tilted-angle standing surface acoustic waves," *Proc. Nat. Acad. Sci. USA*, vol. 111, no. 36, pp. 12992–12997, 2014.
- [20] P. Li *et al.*, "Acoustic separation of circulating tumor cells," *Proc. Nat. Acad. Sci. USA*, vol. 112, no. 16, pp. 4970–4975, 2015.
- [21] F. Guo *et al.*, "Controlling cell–cell interactions using surface acoustic waves," *Proc. Nat. Acad. Sci. USA*, vol. 112, no. 1, pp. 43–48, 2015.
- [22] Y. Ai and B. L. Marrone, "Droplet translocation by focused surface acoustic waves," *Microfluidics Nanofluidics*, vol. 13, no. 5, pp. 715–722, Nov. 2012.
- [23] M. K. Tan, J. R. Friend, and L. Y. Yeo, "Interfacial jetting phenomena induced by focused surface vibrations," *Phys. Rev. Lett.*, vol. 103, no. 2, p. 024501, Jul. 2009.
- [24] T. Frommelt, M. Kostur, M. Wenzel-Schäfer, P. Talkner, P. Hänggi, and A. Wixforth, "Microfluidic mixing via acoustically driven chaotic advection," *Phys. Rev. Lett.*, vol. 100, p. 034502, Jan. 2008.
- [25] S. Collignon, J. Friend, and L. Yeo, "Planar microfluidic drop splitting and merging," *Lab Chip*, vol. 15, no. 8, pp. 1942–1951, 2015.
- [26] J. Friend and L. Y. Yeo, "Microscale acoustofluidics: Microfluidics driven via acoustics and ultrasonics," *Rev. Mod. Phys.*, vol. 83, pp. 647–704, Jun. 2011.
- [27] L. Y. Yeo and J. R. Friend, "Surface acoustic wave microfluidics," *Annu. Rev. Fluid Mech.*, vol. 46, pp. 379–406, Jan. 2014.
- [28] Y. Bourquin, R. Wilson, Y. Zhang, J. Reboud, and J. M. Cooper, "Phononic crystals for shaping fluids," *Adv. Mater.*, vol. 23, no. 12, pp. 1458–1462, Mar. 2011.
- [29] J. Reboud *et al.*, "Shaping acoustic fields as a toolset for microfluidic manipulations in diagnostic technologies," *Proc. Nat. Acad. Sci. USA*, vol. 109, no. 38, pp. 15162–15167, 2012.
- [30] A. Riaud, J.-L. Thomas, E. Charron, A. Bussonnière, O. Bou Matar, and M. Baudoin, "Anisotropic swirling surface acoustic waves from inverse filtering for on-chip generation of acoustic vortices," *Phys. Rev. Appl.*, vol. 4, p. 034004, Sep. 2015.
- [31] A. Riaud, J.-L. Thomas, M. Baudoin, and O. Bou Matar, "Taming the degeneration of Bessel beams at an anisotropic-isotropic interface: Toward three-dimensional control of confined vortical waves," *Phys. Rev. E*, vol. 92, p. 063201, Dec. 2015.
- [32] D. Baresch, J.-L. Thomas, and R. Marchiano, "Observation of a single-beam gradient force acoustical trap for elastic particles: Acoustical tweezers," *Phys. Rev. Lett.*, vol. 116, p. 024301, Jan. 2016.
- [33] A. Riaud, M. Baudoin, J.-L. Thomas, and O. Bou Matar, "Cyclones and attractive streaming generated by acoustical vortices," *Phys. Rev. E*, vol. 90, p. 013008, Jul. 2014.
- [34] M. Tanter, J.-L. Thomas, and M. Fink, "Time reversal and the inverse filter," *J. Acoust. Soc. Amer.*, vol. 108, no. 1, pp. 223–234, Jul. 2000.
- [35] V. Laude, D. Gérard, N. Khelifaoui, C. F. Jerez-Hanckes, S. Benchabane, and A. Khelif, "Subwavelength focusing of surface acoustic waves generated by an annular interdigital transducer," *Appl. Phys. Lett.*, vol. 92, no. 9, p. 094104, 2008.
- [36] M. H. Schoenfish and J. E. Pemberton, "Air stability of alkanethiol self-assembled monolayers on silver and gold surfaces," *J. Amer. Chem. Soc.*, vol. 120, no. 18, pp. 4502–4513, 1998.
- [37] L. Rayleigh, "On the capillary phenomena of jets," *Proc. R. Soc. Lond. A, Math. Phys. Sci.*, vol. 29, p. 94, May 1879.
- [38] A. Qi, L. Y. Yeo, and J. R. Friend, "Interfacial destabilization and atomization driven by surface acoustic waves," *Phys. Fluids*, vol. 20, no. 7, p. 074103, 2008.
- [39] J. Blamey, L. Y. Yeo, and J. R. Friend, "Microscale capillary wave turbulence excited by high frequency vibration," *Langmuir*, vol. 29, no. 11, pp. 3835–3845, 2013.
- [40] C. M. Crudden *et al.*, "Ultra stable self-assembled monolayers of N-heterocyclic carbenes on gold," *Nature Chem.*, vol. 6, no. 5, pp. 409–414, Apr. 2014.
- [41] M. Tanter, J.-F. Aubry, J. Gerber, J.-L. Thomas, and M. Fink, "Optimal focusing by spatio-temporal inverse filter. I. Basic principles," *J. Acoust. Soc. Amer.*, vol. 110, no. 1, pp. 37–47, 2001.
- [42] J.-F. Aubry, M. Tanter, J. Gerber, J.-L. Thomas, and M. Fink, "Optimal focusing by spatio-temporal inverse filter. II. Experiments. Application to focusing through absorbing and reverberating media," *J. Acoust. Soc. Amer.*, vol. 110, no. 1, pp. 48–58, Jul. 2011.
- [43] S. Alzuaga *et al.*, "A large scale X-Y positioning and localisation system of liquid droplet using SAW on LiNbO₃," in *Proc. IEEE Ultrason. Symp.*, vol. 2, Oct. 2003, pp. 1790–1793.
- [44] J. Bennes *et al.*, "Detection and high-precision positioning of liquid droplets using SAW systems," *IEEE Trans. Ultrason., Ferroelectr., Freq. Control*, vol. 54, no. 10, pp. 2146–2151, Oct. 2007.



Antoine Riaud was born in Toulouse, France, in 1989. He received the M.Sc. degree in industrial and chemical engineering conjointly from the École Centrale de Lille, Villeneuve-d'Ascq, France, and Tsinghua University, Beijing, China. He is currently pursuing the Ph.D. degree with the Institut d'Electronique, Microelectronique et Nanotechnologies and the Institut des Nanosciences de Paris, Paris, France.

His current research interests include microfluidics, Lattice-Boltzmann simulation methods, surface acoustic waves actuation of fluids and particles, and quantitative biology.



Michael Baudoin was born in Massy, France, in 1980. He received the M.Sc. degree in mechanical engineering from the École Nationale Supérieure de Techniques Avancées, Palaiseau, France, in 2004, and the M.Sc. degree in fluid mechanics and the Ph.D. degree in fluid mechanics and acoustics from Université Pierre et Marie Curie, Paris, France, in 2004 and 2007, respectively.

He held a postdoctoral position with the LadHyX Laboratory, Ecole Polytechnique, Palaiseau, in 2008. He is currently an Associate Professor with the Université de Lille, Lille, France. His current research interests include the interface between acoustics, microfluidics, and microsystems.



Jean-Louis Thomas was born in Paris, France, in 1966. He received the M.Sc. and Ph.D. degrees in physics with a focus on time reversal mirror from the University of Paris 6, Paris, in 1990 and 1994, respectively.

He was a Researcher with CNRS, Paris, in 1994. Since 2005, he has been with the Institut des Nanosciences de Paris, CNRS, and Université Pierre et Marie Curie, Paris. His current research interests include adaptive focusing in heterogeneous media, nonlinear acoustics, acoustical vortices, and sonoluminescence.



Olivier Bou Matar was born in Villeneuve-sur-Lot, France, in 1970. He received the Ph.D. degree in acoustics from the University of Tours, Tours, France, in 1997.

He joined the Blois Technological Institute, Blois, as an Associate Professor of Electronic and Communication Systems in 1998. Since 2005, he has been a Full Professor with the École Centrale de Lille, Villeneuve-d'Ascq, France. He is currently with the Magnetoacoustics Research Group, Institut d'Electronique, Microelectronique et Nanotechnologies. He is involved with the Joint International Franco-Russian-Ukrainian Laboratory. He has gained great experience in numerical simulation of nonlinear acoustic wave propagation, in the development of ultrasonic imaging systems (nonlinear imaging by magneto-acoustic phase conjugation), and in multiphysics applications involving wave propagation in solids and liquids. He is also the Head of the Acoustical Department with the Institut d'Electronique, Microelectronique et Nanotechnologies, Villeneuve d'Ascq. He has coauthored over 120 international publications in journals and proceedings mainly in the domain of nonlinear acoustic, phononic crystals, and magnetoacoustic. His current research interests include nonlinear magnetoelasticity and magnetostrictive films for microsystems.